Materials Science and Engineering A 486 (2008) 369–375

MATERIALS SCIENCE & ENGINEERING A

www.elsevier.com/locate/msea

Physical models for cleavage fracture at various temperatures—Bases for local approach to fracture of HSLA steel

J.H. Chen *

State Key Laboratory of Gansu Advanced Non-ferrous Metal Materials, Lanzhou University of Technology, Lanzhou 730050, China

Received 27 March 2007; received in revised form 6 September 2007; accepted 7 September 2007

Abstract

The author proposes the critical events controlling cleavage at various temperatures: at a very low temperature (−196 °C), critical event is the nucleation of a crack in ferrite at the precrack tip. At a moderate low temperature (around −100 °C), the critical event is the propagation of a carbide crack into the ferrite grain. With increasing temperature (around DBTT ∼−80 °C), the carbide crack eligible to propagate into the ferrite grain should be the one initiated by a critical strain higher than that to initiate a carbide crack at low temperatures. The higher critical strain increases the flow stress by work hardening for making up the effect of lowering yield stress. At a higher temperature (−30 °C) after the crack tip is blunted to more than 60 μm and a fibrous crack extends, the critical event for cleavage fracture is the propagation of a grain-sized crack.

Keywords: HSLA steel; Cleavage; Physical model; Local approach; Transition temperature

1. Introduction

In 1983, Beremin group [1] indicated that it was possible to model macroscopic fracture in terms of 'local' fracture criteria. They introduced a local parameter, the Weibull stress, providing a basis for probabilistic analysis of fracture. In past 20 years the Beremin model remains the most widely applied statistical micro-mechanical cleavage model. However in recent years some works found difficulties for this model and suggested modified ones [2–6]. The main problem is that based on a single mechanism the Beremin model cannot simulate and explain the sharp upturn of fracture toughness in the ductile-to-brittle transition region (DBTT) by taking into account only the slight lowering of yield stress. In order to modify this model, in Refs. [2–5] authors took into account of the critical plastic strain-criterion for crack nucleation. In Ref. [6], the author considered the conjoint influences of plastic strain and stress triaxiality in the region of the crack tip. These papers related the sharp upturn of fracture toughness to the necessary increase of plastic strain for nucleating an eligible crack nucleus at a carbide particle where accumulated energy was sufficient to drive the crack to propagate into next ferrite grain. The necessary stress triaxiality was needed to limit the region for cleavage triggering. However, these papers have not yet given detailed physical models for cleavage fracture, which are different at various temperatures.

On the variation of the physical models for cleavage with variation of temperatures or acuities of notch (precrack) there are several papers to be referred [17–23]. In Ref. [17] Smith clarified that in developing a realistic physical model of the cleavage process it is of paramount important to ascertain the nature of the critical event in the formation of a cleavage crack, i.e. it is essential to decide if the greatest difficulty in the formation of a crack is its nucleation or whether it occurs at some stage during its growth. In Ref. [18], Oates and Griffiths claimed that in the tensile tests of 3% silicon iron, the critical event for cleavage throughout −196 to −50 °C was the nucleation of a suitable micro-crack. Between −50 and +50 °C the critical event was the growth of grain-size micro-cracks themselves nucleated at cracks in grain boundary carbides or pearlite colonies. The deformation and fracture mechanisms in the notched specimens were in sharp contrast to those described above. Throughout the range −160 to +40 °C twins were not formed at the fracture stress and fracture was determined by the growth of slip-nucleated carbide cracks. The authors attributed the change in the critical event from the growth of ferrite micro-cracks (found in smooth specimens) to the growth of carbide cracks (found in notched specimens) to the difference of high strained volumes in these two types of specimens. In Ref. [19], Lin et al. proposed that

* Tel.: +86 931 2757296; fax: +86 931 2755806.
E-mail address: zchen@lut.cn.

0921-5093/$ – see front matter © 2007 Elsevier B.V. All rights reserved.
doi:10.1016/j.msea.2007.09.012

at the lowest temperature cleavage fracture occurred once the nucleation condition was satisfied. Nucleation dominated behavior would then pertain. At higher temperatures, particles which satisfied the dynamic criterion for propagation across the particle/matrix interface would then become the source of cleavage fracture. At still higher temperatures, the particle might crack and the crack could extend to the first grain boundary without causing failure, stable grain size cracks would then become possible. Within this temperature range, cleavage fracture would occur when a crack could extend dynamically across the ferrite grain boundary. The authors attributed the change in the critical event from crack nucleation (at the lowest temperature) to the carbide crack growth (at higher temperatures) and then to the ferrite grain crack growth at still higher temperatures) to the variation of relative values among the yield stress, carbide cleavage strength and ferrite grain strength at various temperatures. In Ref. [20], Lambert-Perlade et al. suggested the series of variation of the fracture models with temperature as follows:

(1) At very low temperatures fracture is nucleation controlled.
(2) At somewhat higher temperatures failure is controlled by the particle/matrix interface.
(3) At higher temperatures failure is controlled by the strength of matrix/matrix interface.
(4) At even higher temperatures ductile fracture occurs before cleavage cracking could develop into bainitic matrix.

In Ref. [21], Pineau summarized above observations as that this situation observed in one specific steel was likely to be more general. These observations strongly suggested that the micromechanisms operating during fracture toughness measurements at increasing temperature were not the same. In such conditions it would seem preferable to involve a multi-barrier model to account for the temperature dependence of fracture toughness. In author's previous works [22] and [23], the present author proposed that the critical event for the cleavage fracture were different in notched and precracked specimens even if they were made of identical materials. For the notched specimens with the radius of notch roots from 0.075 to 0.45 mm, the critical events for cleavage fracture were the propagation of the ferrite grain-sized micro-cracks (FCs) into the neighboring ferrite grains. However, for the precracked specimens fractured at −110 °C critical events were the propagation of the second particle-sized micro-cracks (SCs) into matrix grains. For the precracked specimens tested at −70 °C, critical events could be the propagations of either SCs or FCs, depending on the blunted width of the precrack prior to the fracture. The cleavage fracture at −196 °C was controlled by the nucleation of the micro-crack.

These results in general are coinciding with the arguments presented in this study.

In this paper, by summarizing results of a series of research work of the present author and his colleagues the models for cleavage fracture at various temperatures are proposed. The adopted general points of view are: (1) cleavage obeys a weakest link principle; (2) cleavage is a dynamic process requiring continuity in a chain of three events: (i) crack nucleation at a second phase particle (carbide); (ii) propagation of the carbide crack into the adjacent matrix grain; (iii) propagation of the grain-sized crack across the boundary into the next grain. In Refs. [7,8] the present author suggested a model for cleavage fracture including three criteria: (i) $\varepsilon_p \geq \varepsilon_{pc}$ for initiating a crack nucleus, here ε_p is the plastic strain, ε_{pc} is its critical value; (ii) $\sigma_m/\sigma_e \geq T_c$ for preventing the nucleated crack tip from blunting, here σ_m is the average principal stress, σ_e is the equivalent stress, σ_m/σ_e presents the stress triaxiality, T_c is its critical value; (iii) $\sigma_{yy} \geq \sigma_f$ for propagating the crack, here σ_{yy} is the principal tensile stress ahead of a precrack, σ_f is the local fracture stress. Because the three criteria should be simultaneously fulfilled at a point where an eligible second phase particle exists, in Ref. [9] the present author supplemented an additional condition for cleavage at moderate low temperatures (around −100 °C). The supplemental condition is that a short crack was initiated, and repeatedly extended and blunted at the fatigue precrack tip. Based on above researches in Ref. [10], the author suggested models for cleavage fracture at various temperatures. In this paper some detailed explanations are supplemented, especially on the mechanism that a higher critical strain for initiating an eligible crack nucleus is needed to gain an increment in the flow stress and the effective shear stress by work hardening for making up the effect of lowering yield stress with increasing temperature. This mechanism can describe the sharp upturn of the fracture toughness in the transition temperature range where the yield stress decreases slightly only.

2. Summary of previous results of investigation on the physical models for cleavage fracture at −196 and −100 °C

Here the results of Refs. [10–13] are summarized and some new figures (Figs. 1 and 2) and ideas are supplemented.

2.1. Physical model for cleavage at −196 °C

Fig. 1 shows the fracture surfaces of specimens fractured at −196 °C. For coarse grains (CG) specimens, cleavage fracture is directly initiated in ferrite at the crack tip (Fig. 1(a)), i.e. $X_f = 0$. For the fine grain (FG) specimen, cleavage fracture can be directly initiated in ferrite at the crack tip (Fig. 1(b)) or at a carbide a distance ahead of the crack tip (Fig. 1(c)). At −196 °C, a high yield stress σ_y is intensified to a very high principle tensile stress σ_{yy} in front of the crack tip (above 2500 MPa), which is sufficient to propagate a carbide crack in common size. The critical event is the initiation of a crack nucleus and can be described by

$$\varepsilon_p \geq \varepsilon_{pc} \quad (1)$$

Fig. 2 shows a schematic of cleavage model at −196 °C, where curve σ_{yy1} describes the distribution of principal stress at a low applied load, curve σ_{yy2} the distribution of principal stress at a high applied load, ε_{p1} the distribution of the plastic strain at the low applied load, ε_{p2} the distribution of the plastic strain at the high applied load, $\sigma_{f(f)}$ the local fracture stress for the propagation of the coarse grain-sized crack, $\sigma_{f(c)}$ the local frac-

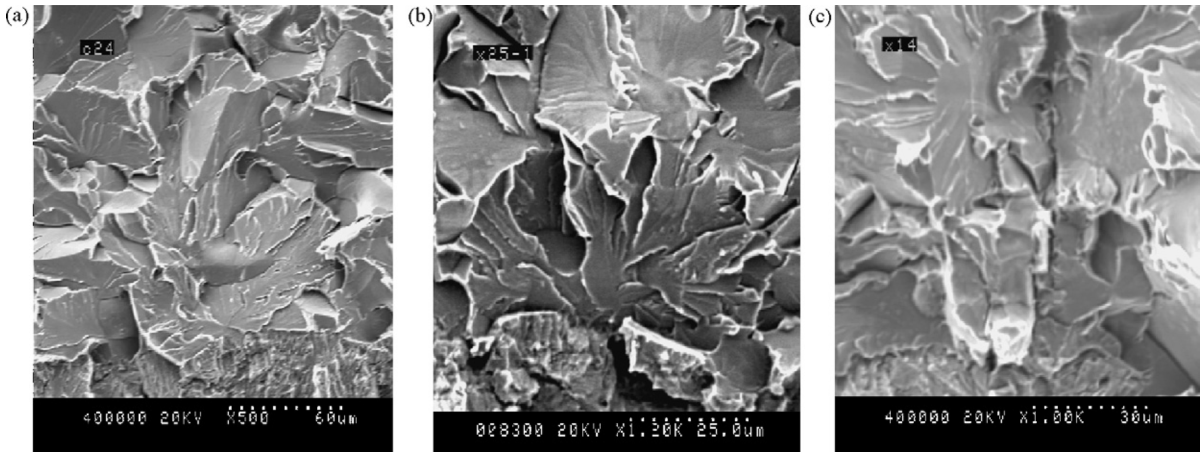

Fig. 1. Fracture surfaces of specimens fractured at −196 °C: (a) CG and (b and c) FG.

ture stress for the propagation of the carbide particle-sized crack, $\varepsilon_{pc(f)}$ the fracture strain for ferrite, and $\varepsilon_{pc(c)}$ is the fracture strain for carbide. As shown by Fig. 2 even at a low applied load, the peak principal stress σ_{yy1} is higher than the local fracture stress of carbide crack $\sigma_{f(c)}$. However, the area where the plastic strain ε_p is higher than the fracture strain of a carbide $\varepsilon_{pc(c)}$ is so narrow that no eligible particle can be found in this area and the crack cannot be triggered. At a high applied load, the principal stress σ_{yy2} just at the precrack tip is higher than the local fracture stress for a coarse grain-sized crack ($\sigma_{f(f)} < 1000$ MPa) and the plastic strain ε_{p2} at the precrack tip reaches the fracture strain of the ferrite grain ($\varepsilon_{pc(f)} \approx 1.4$–$1.8$). For a coarse grain specimen, the crack is initiated in ferrite at the precrack tip and propagated as shown in Fig. 1(a). For fine grain specimens, two cases may happen. The first, in case some carbide particles locate in the close vicinity around the precrack tip, the crack is initiated at the carbide particle ($\varepsilon_{pc(c)} \approx 0.005$) and propagated as shown in Fig. 1(c). The second, in case no carbide crack can be initiated ahead of the precrack tip, the crack is initiated in ferrite at the precrack tip ($\varepsilon_{pc(f)} \approx 1.4$–$1.8$) and propagated at $\sigma_{f(f)} \approx 1070$ MPa (as shown in Fig. 1(b)). Therefore in Table 2, both σ_f and ε_{pc} for FG have two values, corresponding to $\sigma_{f(f)}/\sigma_{f(c)}$ and $\varepsilon_{pc(f)}/\varepsilon_{pc(c)}$. Because the critical event for cleavage is the nucleation of crack, the measured $\sigma_{f(f)}$ and $\sigma_{f(c)}$ may be higher than the real values.

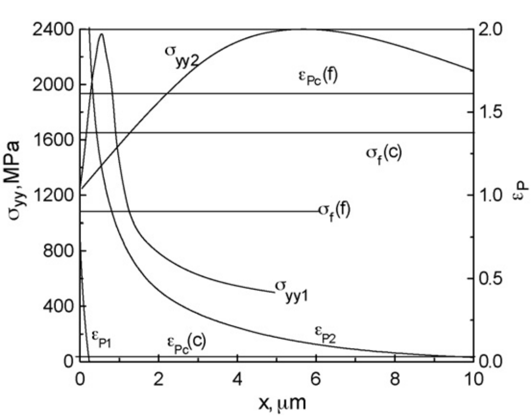

Fig. 2. A schematic of cleavage model at −196 °C.

2.2. *Physical model for cleavage at around −100 °C*

The physical model of cleavage at around −100 °C has been thoroughly investigated [7–9]. Based on the fact that remaining cracks are observed in boundary carbides (as seen in Fig. 3), it is concluded that the critical event for cleavage at around −100 °C is identified as the propagation of a crack, which initiates in a carbide, into the ferrite grain. Three criteria mentioned in introduction for triggering cleavage fracture are $\varepsilon_p \geq \varepsilon_{pc}$, $\sigma_m/\sigma_e \geq T_c$ and $\sigma_{yy} \geq \sigma_f$. However, as shown in Fig. 4(a) for a precracked specimen if the crack tip is only blunted, the region left to line I, where the criterion $\varepsilon_p \geq \varepsilon_{pc}$ is satisfied for initiating a crack nucleus and the region right to line P, where the criteria $\sigma_m/\sigma_e \geq T_c$ and $\sigma_{yy} \geq \sigma_f$ are satisfied for propagating the crack, are separated by a distance *X*. The crack which is just nucleated cannot be propagated and cleavage cannot be triggered. This is the reason why in a precracked specimen the cleavage fracture cannot be carried out at a lower applied load even though a suffi-

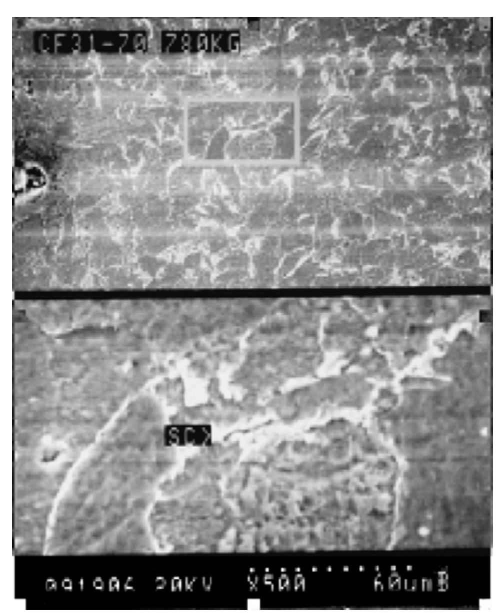

Fig. 3. Remaining carbide crack [7].

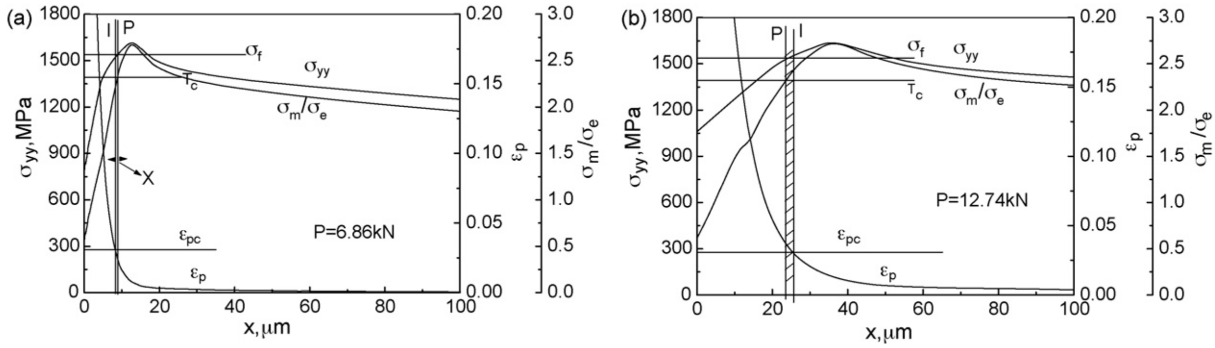

Fig. 4. Schematic of fracture model at around −100 °C. (a) Precrack tip is only blunted. The region where $\varepsilon_p \geq \varepsilon_{pc}$ (left to line I) and the region where $\sigma_m/\sigma_e \geq T_c$ (right to line P) are separated by a distance X_s. (b) After a short crack is initiated, and repeatedly extended and blunted at the precrack tip. The region where $\varepsilon_p \geq \varepsilon_{pc}$ and the region where $\sigma_m/\sigma_e \geq T_c$ (or $\sigma_{yy} \geq \sigma_f$) are overlapped each other [9].

cient normal stress σ_{yy} has existed which is higher than the local fracture stress σ_f. Ref. [9] discussed the process making these separated regions overlapped by supplementing an additional condition that a short crack is initiated, and repeatedly extended and blunted at the fatigue precrack tip. At a critical applied load the short crack is extended and blunted to a certain size and the blunted precrack tip is re-sharpened. The stress and strain fields are rebuilt. While the strain remains, the distribution of the stress moves closer to the precrack tip and makes the regions satisfying the three criteria overlapped (shown in Fig. 4(b)). An active region (shaded) is created where three criteria are simultaneously satisfied and cleavage could be triggered.

With increasing temperature the yield stress decreases, the principal stress σ_{yy} will decrease and the line P in Fig. 4(b) will move to right. It makes the overlap of these regions more difficult. It is the reason why the fracture toughness increases with temperature in the temperature range of the lower shelf.

3. Physical model for cleavage in transition temperature range around (−80 to −30 °C)

3.1. Materials

The materials used are C–Mn steels, the range of compositions of these steel is shown in Table 1. The specimens were austenized at 1250 °C for 3 h, which were then cooled in furnace to obtain coarse ferrite grains with pearlite colonies and few particles of carbides. The fine grain specimens were produced by austenizing at 900 °C for 45 min then cooled in furnace.

Table 1
Range of compositions of used C–Mn steel

C	0.13–0.16
Si	0.31–0.33
Mn	1.34–1.44
S	0.012–0.016
P	0.015–0.023

Two groups of specimens with fine ferrite grain yet various carbide sizes were obtained by austenizing at 900 °C for 45 min then air-cooled. The coarse carbide particles were obtained by spheroidizing at 700 °C for 120 h and the fine carbide particles for 24 h. For the group of coarse grains (CG), the average grain size is 55 μm and the coarsest is 80 μm in sizes. The corresponding sizes for the fine grain (FG) group are 30 and 40 μm. Other two groups of specimens have the coarsest grain sizes of 20 μm and coarsest carbide particles of 2.4 μm (SC) and 3.6 μm (LC), respectively.

3.2. Measured macroscopic and microscopic parameters by standard COD bending tests

The average values of the measured macroscopic and microscopic parameters are shown in Tables 2 and 3. In Tables 2 and 3, all specimens were finally fractured by cleavage. From these values, it is confirmed that with temperature increasing the fracture toughness (COD, δ_c) increases. Especially in the range above −100 °C the fracture toughness has a sharp upturn. The distance, X_f, of the cleavage initiation site from the crack tip increases from

Table 2
Macro and microscopic parameters measured by COD tests of specimens CG and FG

Specimen	Grain size (μm) (Ave/max)	T (°C)	σ_y (MPa)	δ_c (μm)	X_f (μm)	σ_f (MPa)	ε_{pc}
		−196	353	3.17	0	999.8	1.64
CG	55/80	−110	379	11.78	19.36	1626	0.0253
		−30	287	216.7	190.3	1193	0.122
		−196	801	2.90	0/3.31	1070/2333	1.62/0.0056
FG	30/40	−110	435	29.61	21.04	1608	0.0923
		−80	411	357.8	587		

CG: coarse grains; FG: fine grain; σ_y: yield stress; δ_c: value of crack opening displacement (COD); X_f: distance of cleavage initiation site from the crack tip; σ_f: local fracture stress; ε_{pc}: fracture strain.

Table 3
Macro and microscopic parameters measured by COD tests of specimens LC and SC

Specimen	Grain size max (μm)	Carbide size max (μm)	T (°C)	σ_y (MPa)	δ_c (μm)	X_f (μm)	σ_f (MPa)	ε_{pc}
			−196	755	3.0	8		0.0091
LC	20	3.6	−100	425	22	46	1598	0.020
			−90	420	44	58	1613	0.039
			−196	770	3.5	13		0.0047
SC	20	2.4	−100	450	59	83	1712	0.032
			−90	420	92	89	1644	0.046

σ_y: yield stress; δ_c: value of crack opening displacement (COD); X_f: distance of cleavage initiation site from the crack tip; σ_f: local fracture stress; ε_{pc}: fracture strain.

tens microns at −110 °C to hundreds microns after a fibrous crack extends. This phenomenon characterizes the change of cleavage fracture from being triggered in a precracked specimen to being triggered in a notched specimen. More interesting, the fracture strains, which were measured at the fracture initiation sites increased with test temperatures increasing.

3.3. For the first stage (around DBTT ∼−80 °C)

In this temperature range, the criteria controlling cleavage fracture are the same as that at −100 °C. However, with temperature increasing, the yield stress decreases to make the peak principal stress σ_{yy} being lower than the local fracture stress $\sigma_{f(c)}$. In this case, the Smith's formula [14] can be used to analyze the process. Formula of Smith is

$$\left(\frac{C_0}{d}\right)\sigma_f^2+\tau_{eff}^2\left\{1+\frac{4}{\pi}\left(\frac{C_0}{d}\right)^{1/2}\frac{\tau_i}{\tau_{eff}}\right\}^2 \geq \frac{4E\gamma_p}{\pi(1-\nu^2)d} \qquad (2)$$

where C_0 is the thickness of carbide, d the grain diameter, σ_f the local fracture stress, $\tau_{eff}=\tau_y-\tau_i$ the effective shear stress, τ_y the yield shear stress, τ_i the friction shear stress, υ the Poisson's ratio, and γ_p is the effective surface energy.

Here, σ_f is taken as the value of the principal stress σ_{yy}, which is established by intensifying the yield stress σ_y in front of the precrack tip, $\sigma_f=\sigma_{yy}=Q\sigma_y$. Q is the intensification factor. With temperature increasing, the yield stress σ_y decreases, then the σ_{yy} decreases. For compensation, the σ_y (work hardened to σ_{flow} analyzed in Ref. [15]) and the τ_{eff} should be increased to make up the driving force reaching the local fracture stress for a carbide crack $\sigma_{f(c)}\approx 1600$ MPa. It means that the carbide crack eligible to propagate into the ferrite grain should be the one initiated by a fracture strain higher than that to initiate a carbide crack at low temperatures. The higher fracture strain increases the flow stress σ_{flow} and the effective shear stress τ_{eff} by work hardening for making up the effects of lowering the yield stress. This is just the case shown in Tables 2 and 3 that with temperature increasing the measured fracture strain increases. The mechanism of compensating the effect of lowering the yield stress by work hardening is schematically shown in Fig. 5. As shown in Fig. 5 the gradient of raising flow stress by work hardening is low (Fig. 5, line 2). For compensating a slight reduce in yield stress with increasing temperature (Fig. 5, line 1) a certain amount of plastic strain ε_p is needed to be developed (Fig. 5, lines 2 and 3). This is just the reason why a sharp upturn (DBTT) of the fracture toughness (Fig. 5, line 4) in the ductile-to-brittle transition region results from only a slight lowering of yield stress (Fig. 5, line 1).

3.4. For the second stage at a higher temperature (−30 °C)

Fig. 6 shows a region around the tip of a fibrous crack, which extends from the precrack tip of a CG specimen tested at −35 °C. There are many remaining micro-cavities mixed with micro-cracks in boundary carbides and several grain-sized cracks. Based on previous work [7,10,12] and Fig. 6, it is suggested that in this temperature range the critical event for cleavage fracture is changed from the propagation of a carbide-sized crack to the propagation of a grain-sized crack after the precrack tip is blunted to more than 60 μm and a fibrous crack extends.

The change of the fracture model can be explained as follows:

For the second stage at a higher temperature (−30 °C), in order to reach the necessary fracture strain at eligible carbide, the applied load makes the strain at the precrack tip being higher than that for ferrite grain fracture. The precrack tip is blunted to more than 60 μm and a fibrous crack is extended. In this stage the critical event for cleavage changes from the propagation of a carbide-sized crack to the propagation of the grain-sized crack as shown by several retaining grain-sized cracks in Fig. 6. Fig. 7 shows the schematics explaining the change of critical event for

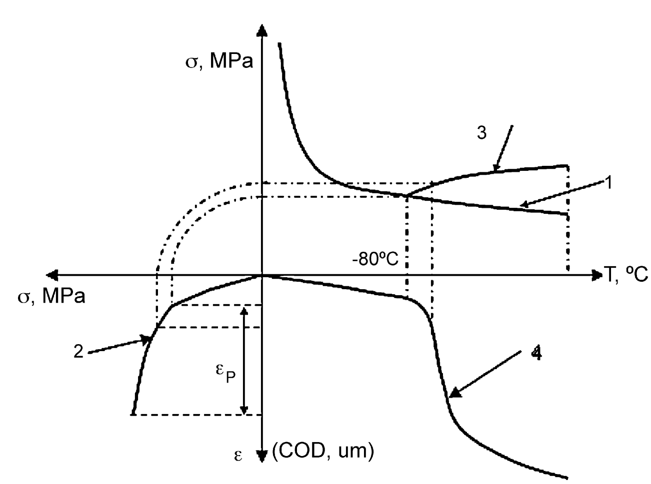

Fig. 5. Schematic explaining the effect of increasing fracture strain: line 1, σ_y–T; line 2, σ_{flow}–ε_p; line 3, stress compensation; line 4, COD–T.

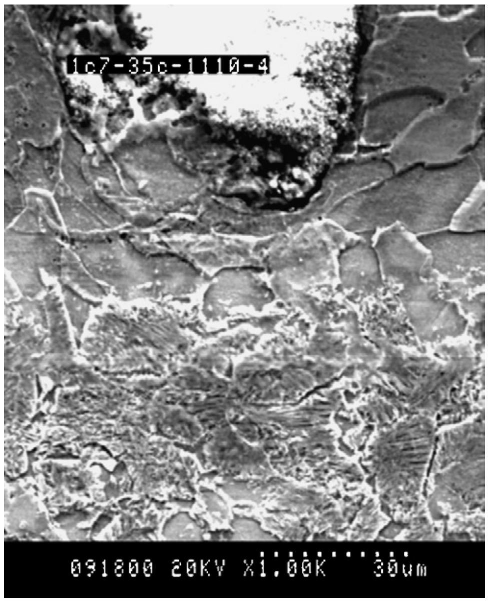

Fig. 6. Vicinity around an extending crack.

cleavage fracture where $\sigma_{yt} = \sigma_n$ is the normal stress induced by the dislocation pile-up, σ_{yy} the principal stress combined by the stress intensified in front of the precrack σ_{yy} with the σ_{yt}, $\sigma_{f(c)}$ the fracture stress for propagating a carbide-sized crack across the boundary between the particle and the ferrite grain, and $\sigma_{f(f)}$ is the fracture stress for propagating a grain-sized crack across the boundary between the ferrite grains.

Because a wide field of high strain is established, it is not difficult for the normal stress induced by the dislocation pile-up in conjunction with the applied principal stress to drive the carbide crack into ferrite grain. However, according to the following formula of Stroh [16], the normal stress induced by the dislocation pile-up is of a short distance-acting stress.

$$\sigma_n = \frac{2}{3}\left[\sigma_y\left(\frac{L}{r}\right)^{1/2}\right] \quad (3)$$

where σ_n is the normal stress induced by dislocation pile-up, σ_y the yield stress, L the half length of grain, and r is the distance from the edge of the dislocation pile-up.

In the case of a carbide which is very thin ($L/r = 10$–20), the normal stress σ_n induced by the dislocation pile-up combined with the applied principal stress is sufficient to drive a carbide crack into the ferrite grain (as shown by the peak on the curve σ_{yy} in Fig. 7). However, the action distance of normal stress induced by the dislocation pile-up is too short to effectively extend the crack across the boundary of next grain ($L/r = 0.5$) (right sector of the curve σ_{yy} in Fig. 7). With the extension of the crack (increasing r in Eq. (3)), the driving force σ_n in Eq. (3) decreases (in Fig. 7 the σ_{yt} decreases). This is the difference between a Griffiths crack and a dislocation pile-up-driven crack.

In case, the yield stress is remarkably reduced with the temperature increasing, the σ_{yy} at the boundary of the second grain may be lower than the $\sigma_{f(f)}$, the local fracture stress for the ferrite grain. In this case, the boundary between grains becomes the main barrier for crack propagation. This is the reason why in this temperature range the critical event for cleavage fracture is changed from the propagation of a carbide-sized crack to the propagation of a grain-sized crack (Fig. 7). The criterion for cleavage fracture is $\sigma_{yy} \geq \sigma_{f(f)} < 1000$ MPa. The increase of toughness results from the extension of fibrous crack, which is terminated by the triggering of the cleavage crack. The higher the temperature, the longer the fibrous crack, the higher the toughness.

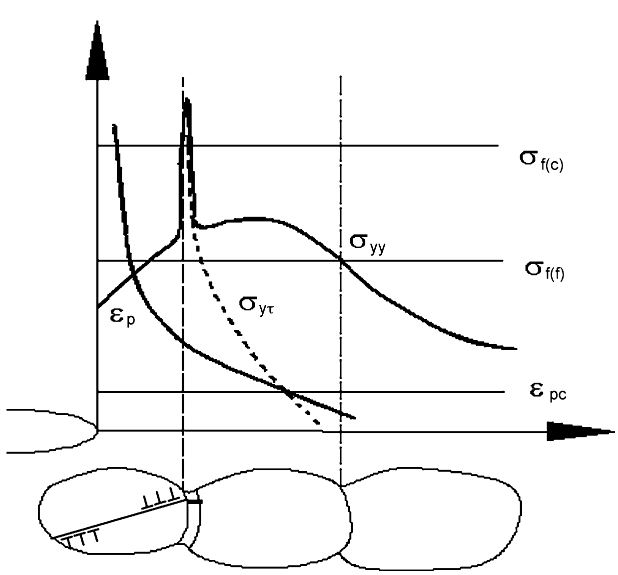

Fig. 7. Schematics explaining the change of critical event for cleavage fracture from the propagation of a carbide-sized crack to the propagation of a grain-sized crack.

4. Physical model for cleavage in upper shelf

At a temperature of upper shelf, the normal stress σ_{yy} is never higher than the local fracture stress σ_f, the cleavage fracture will never happen. Specimens are fractured by fibrous cracking-ductile failure.

Because the fibrous crack stretches through all ligament of the specimen and its length keeps an approximately constant value, the fracture toughness does not vary markedly with further increasing of temperature.

5. Conclusion

Based on author's previous work of a general model for cleavage fracture: three criteria, $\varepsilon_p \geq \varepsilon_{pc}$ for initiating a crack nucleus; $\sigma_m/\sigma_e \geq T_c$ for preventing the nucleated crack tip from blunting; $\sigma_{yy} \geq \sigma_f$ for propagating the crack, should be satisfied simultaneously at a site where a eligible weakest constituent locates, the author proposes the critical events controlling cleavage at various temperatures.

(1) At a very low temperature (−196 °C), critical event is the nucleation of a crack in ferrite at the precrack tip or at a carbide particle.

(2) At a moderate low temperature (around −100 °C), the critical is the propagation of a crack initiated at a carbide into the ferrite grain.
(3) With temperature increasing (around DBTT ∼−80 °C), the carbide crack eligible to propagate into the ferrite grain should be the one initiated by a critical strain higher than that to initiate a carbide crack at low temperatures. The higher critical strain increases the flow stress and the effective shear stress by work hardening for making up the effect of lowering yield stress. This is just the reason why a sharp upturn (DBTT) of the fracture toughness in the ductile-to-brittle transition region results from only a slight lowering of yield stress.
(4) At higher temperature (around −30 °C), after the crack tip is blunted to more than 60 μm and a fibrous crack extends, the critical event for cleavage fracture is the propagation of a grain-sized crack.
(5) Following the change of critical events, the critical values of above three criteria also change with temperature.

Acknowledgements

This work was financially supported by the National Nature Science Foundation of China (nos. 50671047 and 50471109), National Hi-tech Research and Development Program of China (863 Program) (2006AA03A206) and Foundation for Doctorate of Education Ministry (20060731001). Authors would like to thank Miss Martha Ello for help in English formatting.

References

[1] F.M. Beremin, Metall. Trans. A 14 (1983) 2277–2287.
[2] B.Z. Magolin, V.A. Shvetsva, G.P. Karzov, Int. J. Pres. Ves. Pip. 72 (1997) 73–87.
[3] P. Hausild, C. Berdin, P. Bompard, Mater. Sci. Eng. A 391 (2005) 188–197.
[4] S.R. Bordet, A.D. Karstensen, D.M. Knowles, C.S. Wiesner, Eng. Fract. Mech. 72 (2005) 435–452.
[5] S.R. Bordet, A.D. Karstensen, D.M. Knowles, C.S. Wiesner, Eng. Fract. Mech. 72 (2005) 453–474.
[6] X. Gao, G. Zhan, T.S. Srivatsan, Mater. Sci. Eng. A 394 (2005) 210–219.
[7] J.H. Chen, G.Z. Wang, Metall. Trans. A 23 (1992) 509–517.
[8] J.H. Chen, C. Yan, J. Sun, Acta Metall. Mater. 42 (1994) 251–261.
[9] J.H. Chen, Q. Wang, G.Z. Wang, Z. Li, Acta Mater. 51 (2003) 1841–1855.
[10] S.R. Yu, Z.G. Yan, R. Cao, J.H. Chen, Eng. Fract. Mech. 73 (2006) 331–347.
[11] G.Z. Wang, J.H. Chen, Metall. Trans. A 27 (1996) 84–92.
[12] S.R. Yu, Dissertation paper for doctorate degree, Lanzhou University of Technology, 2005.
[13] Z.G. Yan, Dissertation paper for master degree, Lanzhou University of Technology, 2004.
[14] E. Smith, Proceedings of Conference on the Physical Basis of Yield and Fracture, Physical Society, Oxford, 1966, pp. 36–54.
[15] N.J. Petch, R.W. Armstrong, Acta Metall. 37 (1989) 2279–2285.
[16] A.N. Stroh, Adv. Phys. 6 (1957) 418–463.
[17] E. Smith, Int. J. Fract. Mech. 14 (1968) 131–146.
[18] G. Oates, J.R. Griffiths, Metal Sci. J. 3 (1969) 111–115.
[19] T. Lin, A.G. Evens, R.O. Ritchie, Metall. Trans. A 18 (1987) 641–651.
[20] A. Lambert-Perlade, A.F. Gourgues, J. Besson, T. Sturel, A. Pineau, Metall. Mater. Trans. A 35 (2004) 1039–1053.
[21] A. Pineau, Int. J. Fract. 138 (2006) 139–166.
[22] J.H. Chen, G.Z. Wang, H. Ma, Metall. Trans. A 21 (1990) 321–330.
[23] J.H. Chen, L. Zhu, G.Z. Wang, Z. Wang, Metall. Trans. A 24 (1993) 132–140.